

1 Supplementary material for LHCb-PAPER-2021-030

This appendix contains supplementary material that will be posted on the public CDS record but will not appear in the paper.

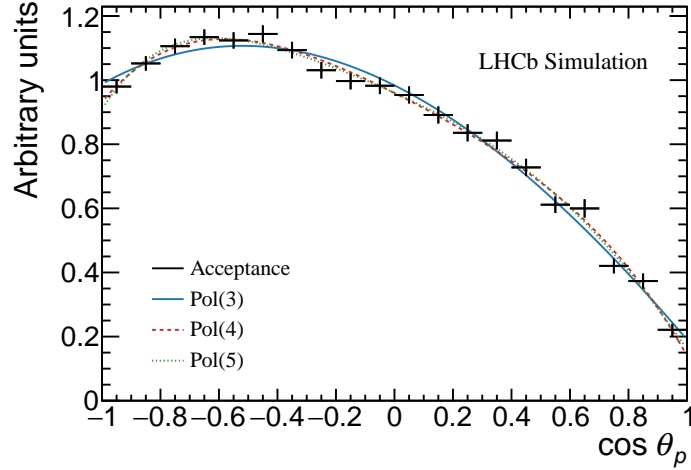


Figure 1: Angular acceptance computed from $\Lambda_b^0 \rightarrow \Lambda \gamma$ simulation as the ratio between the angular distribution after reconstruction and full selection and at generator level. The simulation is represented by the black markers and the results of fits with polynomials of orders 3, 4 and 5 with solid blue, dashed red and dotted green lines, respectively. The polynomial of order 4 is used for the nominal model and alternative models are obtained using polynomials of order 3 and 5.

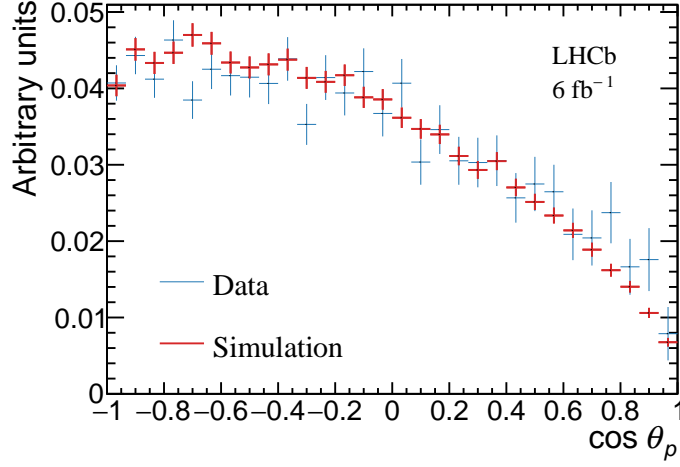


Figure 2: Angular acceptance computed from $\Lambda_b^0 \rightarrow \Lambda J/\psi$ data (blue) and simulation (red). In data, the distribution after the full selection is divided by the theoretical distribution using the parameters measured by LHCb in Ref. [?]. In simulation, events are generated according to the available phase space and the acceptance shape is directly computed from fully reconstructed and selected decays.

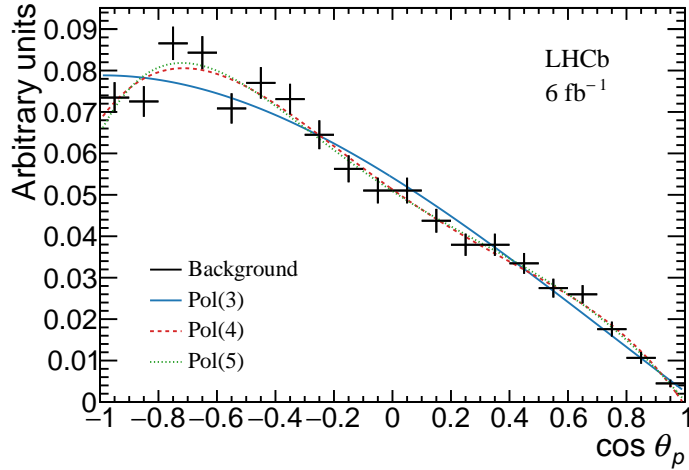


Figure 3: Proton angular distribution, $\cos \theta_p$, for background candidates in the Λ_b^0 invariant mass sidebands. The data are represented by the black markers and the results of fits with polynomials of orders 3, 4 and 5 with solid blue, dashed red and dotted green lines, respectively. The polynomial of order 4 is used for the nominal model and alternative models are obtained using polynomials of order 3 and 5.

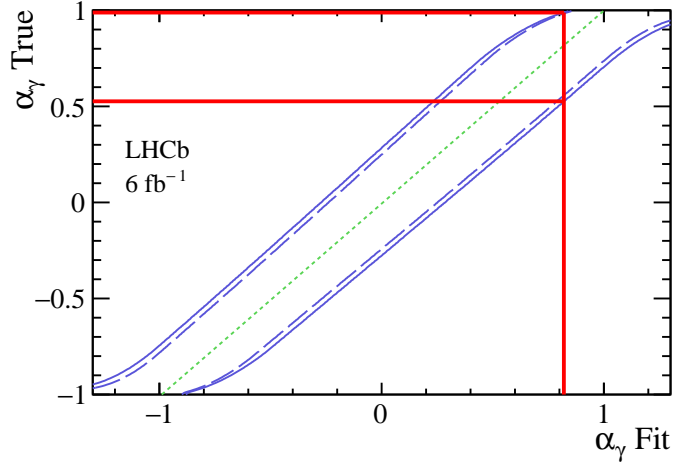


Figure 4: One-sigma confidence intervals on α_γ computed with the Feldman-Cousins technique within the physical limits of this parameter. The dotted green line gives the relation between the central value measured by the fit and the true value, while the blue lines represent the 68% confidence intervals including statistical (dashed) and statistical and systematic (solid) uncertainties. The red vertical line indicates the central value measured by the fit and the horizontal ones the derived 68% confidence interval.

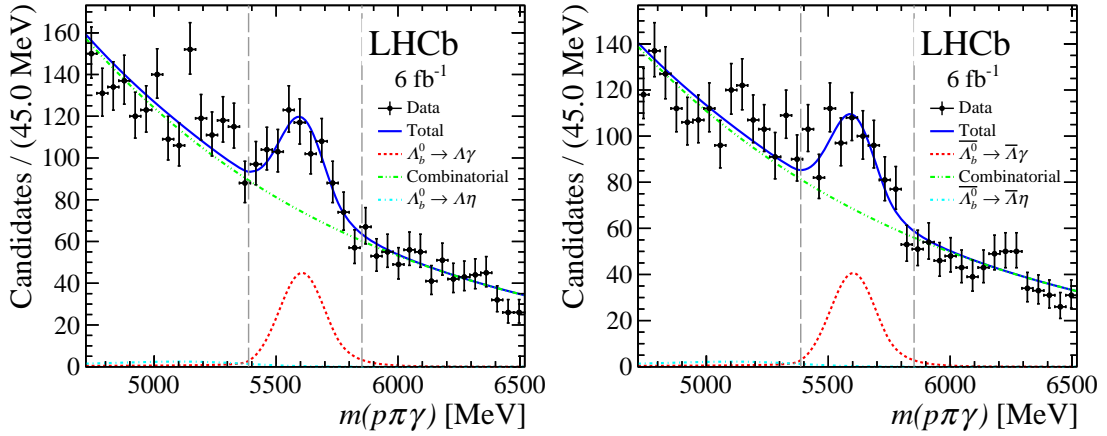


Figure 5: Invariant-mass distribution, $m(p\pi\gamma)$, of selected (left) $\Lambda_b^0 \rightarrow \Lambda\gamma$ and (right) $\bar{\Lambda}_b^0 \rightarrow \bar{\Lambda}\gamma$ candidates. The data are represented by black points and the result of the fit by a solid blue curve while signal, combinatorial and $\Lambda_b^0 \rightarrow \Lambda\eta$ contributions are represented by the dotted red, green and blue curves, respectively.

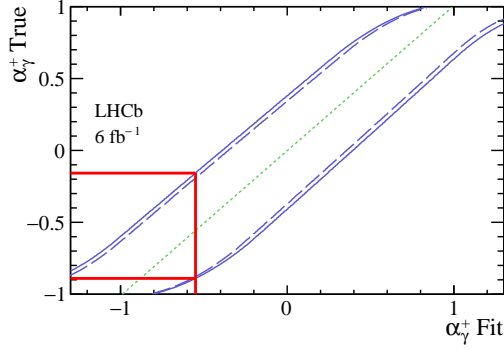


Figure 6: One-sigma confidence interval on α_γ^+ computed with the Feldman-Cousins technique within the physical limits of this parameter. The green dotted line is the relation between the central value measured by the fit and the true value, while the blue lines are the 68% confidence intervals including statistical (dashed) and statistical and systematic (solid) uncertainties. The red vertical line is the central value measured by the fit and the horizontal lines are the derived 68% confidence interval.

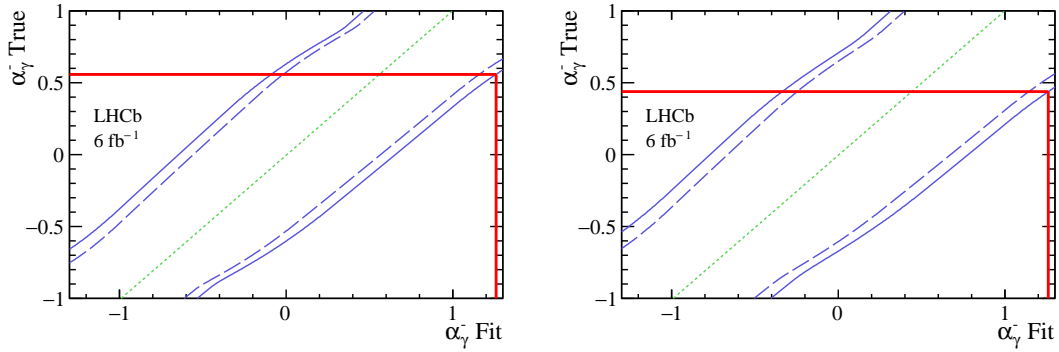


Figure 7: Confidence intervals on α_γ^- with the Feldman-Cousins technique within the physical limits of this parameter. The dotted green line is the relation between the central value measured by the fit and the true value, while the blue lines are the 90% (left) and 95% (right) confidence intervals including statistical (dashed) and statistical and systematic (solid) uncertainties. The red vertical line is the central value measured by the fit and the horizontal lines are the derived confidence interval.